ORIGINAL ARTICLE

Correcting GPS measurements for non-tidal loading

Anthony Mémin[1] · Jean-Paul Boy[2] · Alvaro Santamaría-Gómez[3]

Abstract

Non-tidal loading (NTL) deforms the earth's surface, adding variability to the coordinates of geodetic sites. Yet, according to the IERS Conventions, there are no recommended surface-mass change models to account for NTL deformation in geodetic position time series. We investigate the NTL signal recorded at 585 GPS stations at different frequency bands, from day to years, by comparing GPS estimated displacements to modeled environmental loading. We used up-to-date and high-resolution (both temporal and spatial) models to account for NTL induced by mass changes in the atmosphere, oceans, and continental hydrology. Vertical land motions variability is reduced on average by up to 20% when correcting the series for non-tidal atmospheric and oceanic loading, employing either barotropic or baroclinic ocean models. We then focus on characterizing the ocean response to air-pressure variations, and we observe that there are no significant differences at seasonal timescales between a barotropic ocean model forced by air pressure and winds and a more classical baroclinic ocean model forced by wind, heat and freshwater fluxes. However, any of these choices further reduces the variability by 5% compared to the classical static inverted barometer ocean response. The variability of the vertical coordinate changes is further reduced by an additional 5% by also correcting for continental hydrology loading, especially at seasonal periods. For horizontal coordinate changes, the variability is reduced by less than 5% after correcting for all studied surface-mass changes.

Keywords GPS · Non-tidal loading · Vertical land motion · Deformation

Abbreviation

ACC	Antarctic Circumpolar Current
CF	Center of figure
D-NTAOL	Dynamic non-tidal atmospheric and oceanic loading
DORIS	Doppler orbitography and radiopositioning integrated by satellite
ECCO	Estimating the Circulation and Climate of the Ocean
ECWMF	European Centre for Medium-Range Weather Forecasts
ELM	East land motion
GCM	General circulation model
GLDAS	Global Land Data Assimilation System
GLORYS	Global Ocean ReanalYsis and Simulation
GPS	Global Positioning System
IB	Inverted barometer
IERS	International Earth Rotation and Reference Systems Service
MERRA	Modern Era Retrospective-Analysis
NCEP	National Centers for Environmental Prediction
NLM	North land motion
NTAL	Non-tidal atmospheric loading
NTAOL	Non-tidal atmospheric and oceanic loading
NTL	Non-tidal loading
NTOL	Non-tidal oceanic loading
OGCM	Ocean general circulation model
RMS	Root mean square
SLR	Satellite laser ranging
STD	Standard deviation
TUGO-m	Toulouse Unstructured Grid Ocean model
VLBI	Very long baseline interferometry
VLM	Vertical land motion
WRMS	Weighted root mean square

✉ Anthony Mémin
anthony.memin@univ-cotedazur.fr

1 Université Côte d'Azur, CNRS, Observatoire de la Côte d'Azur, IRD, Géoazur, 250 rue Albert Einstein, 06560 Valbonne, France

2 IPGS (UMR 7516), EOST/Université de Strasbourg, CNRS, 5 rue René Descartes, 67084 Strasbourg cedex, France

3 GET, Université de Toulouse, CNES, CNRS, IRD, UPS, 14 avenue Edouard Belin, Toulouse 31400, France

Introduction

The global circulation of the oceans, the atmosphere, melting of glaciers and ice sheets, continental hydrology, oceanic tides, earthquakes, or human activities (e.g., water pumping) induce changes in the global distribution of mass at the earth's surface. In response to the sub-daily to inter-annual non-tidal redistribution of air, water, and snow masses, namely mass changes that are not due to gravitational forces exerted by planetary bodies or the sun and that we call here-after non-tidal loading (NTL), the surface of the solid earth deforms elastically. It can theoretically reach up to 30 mm in the vertical direction at seasonal timescales (van Dam and Wahr 1987; van Dam et al. 2001; Schuh et al. 2003). More prolonged mass changes such as the thinning of glaciers are characterized by viscous deformation at longer periods (Mémin et al. 2014a).

Surface displacements resulting from NTL has already been detected using several geodetic techniques such as Very Long Baseline Interferometry (VLBI, van Dam and Herring 1994; Eriksson and Mac Millan 2014; MacMillan and Gipson 1994; Petrov and Boy 2004; Tesmer et al. 2009; Krásná et al. 2015), Global Positioning System (GPS, van Dam et al. 1994, 2001, 2012; Davis et al. 2004; Gégout et al. 2010; Tesmer et al. 2009; Tregoning and van Dam 2005; Tregoning and Watson 2009), Doppler orbitography and radiopositioning integrated by satellite (DORIS, Mangiarotti et al. 2001), or Satellite Laser Ranging (SLR, Sósnica et al. 2013). As a consequence, surface displacements induced by NTL have been extensively investigated by studying the different contributions either individually, separating the non-tidal atmospheric loading (NTAL, van Dam and Wahr 1987; van Dam and Herring 1994; van Dam et al. 1994; MacMillan and Gipson 1994; Tregoning and van Dam 2005; Tregoning and Watson 2009, 2011), the non-tidal oceanic loading (NTOL, van Dam et al. 2012; Fratepietro et al. 2006; Geng et al. 2012; Mémin et al. 2014b; Williams and Penna 2011), and the hydrological loading (van Dam et al. 2001, 2007; Davis et al. 2004; Tregoning et al. 2009), or simultaneously (Gégout et al. 2010; Jiang et al. 2013; Mangiarotti et al. 2001; Schuh et al. 2003; Sósnica et al. 2013; Santamaría-Gómez and Mémin 2015). It results that applying NTL corrections either a posteriori or at the observation level (Boehm et al. 2009; Gégout et al. 2010; Krásná et al. 2015; Tregoning and van Dam 2005) reduces the variability of the geodetic time series, especially the seasonal variations (Gégout et al. 2010). Seasonal signals have the largest amplitude and propagate into the estimation of the translation and scale parameters that are used to generate a terrestrial reference frame as well as into earth rotation parameters (Collilieux et al. 2010; Krásná et al. 2015).

Significant changes also occur at high frequencies, such as the storm surge event observed along the coast of the North Sea in sub-daily GPS time series (Geng et al. 2012). Such an event may induce sub-daily vertical motion up to 30 mm (Fratepietro et al. 2006; Mémin et al. 2014b). Correcting for NTOL can improve GPS height time series repeatability (Williams and Penna 2011) and would likely enable detecting other crustal motion at the sub-millimeter per year level.

Recently, it has been shown that NTL effects can bias estimates of geodetic vertical velocity by 0.5 mm/yr over the continent to more than 1 mm/yr in the southern tropical regions (Santamaría-Gómez and Mémin 2015). It is five to more than ten times larger than the requirement of the Global Geodetic Observing System (Plag et al. 2009) on inter-annual to secular timescales. Geodetic techniques require accurate global circulation models to allow precise estimation of the earth's surface displacements, to reduce the variability of position time series, and finally to improve the geophysical interpretation of their residuals. It would also lead to a better understanding of other sources of uncertainties. However, there is yet no recommendation from the International Earth Rotation and Reference Systems Service (IERS) (Petit and Luzum 2010) for using models that would provide a good representation of the surface-mass changes in geodetic observations. It is partly because we still do not have a comprehensive understanding of the full observed signal, and there is no consensus regarding which models should be used, and how to model the ocean response to pressure forcing.

As a result, the effects of NTL have already been observed in geodetic time series, occur in a wide range of periods, and have an impact on crustal velocity estimates and the realization of the terrestrial reference frame. A better understanding of NTL contribution to geodetic time series will lead to the recommendation about models to be used to remove it from the time series so that the effects mentioned above will be reduced. It will also make it possible to investigate geophysical processes that have smaller effects. Hence, we compare the effects of environmental loading signal into current GPS observations using the contribution from various global circulation models for the atmosphere, the ocean and continental hydrology. We especially focus on the ocean response to air-pressure forcing using two baroclinic ocean models, forced by winds, head, and freshwater, and one barotropic ocean model, forced by air pressure and winds, that are usually assumed to represent different frequencies of the ocean variability.

We characterize the NTL signals recorded by GPS within several frequency bands. We consider all major environmental contributions from daily variations and use up-to-date and high-resolution models of surface-mass transport to compute the vertical land motion (VLM) at geodetic sites.

After a short description of the models and the data we use, we present our results and give concluding remarks.

Loading models

In this section we introduce the strategy employed to compute the land motion induced by surface-mass changes. We provide a comprehensive description of the models of surface-mass transport that we use, and we characterize the resulting VLM. We specifically separate our analysis according to several frequency bands that reflect different physical behavior of the atmosphere, the ocean and the continental hydrology.

Computing loading effects

Surface displacements due to atmospheric, oceanic and hydrological loading can be computed using the general circulation model (GCM) outputs convolved with the appropriate Green's functions. The latter describes the earth's elastic response to surface loads by taking into account its average mechanical properties (Farrell 1972; Petrov and Boy 2004; Mémin et al. 2009). Differences between using various earth models are negligible on a global scale, typically less than 2% (Petrov and Boy 2004). Surface displacements are computed in a reference frame for which the origin is the center of figure (CF) of the earth (Blewitt 2003).

For all the loading computations, a high-resolution land/sea mask is required, especially for coastal or island stations. We choose a resolution equal to or higher than the native model grids, namely a resolution of 0.25° for NTOL and hydrological loading estimates, and 0.10° for NTAL. Indeed, the atmospheric pressure is a continuous field over the entire surface of the earth so we can interpolate to 0.10° and therefore use a refined land/sea mask to compute the ocean response with the inverted barometer hypothesis (see the following subsection). It is not possible to perform a similar interpolation for mass changes in the ocean and for the soil-moisture and snowfields as they may depend, for example, on the wavelength of soil parameters. Thus, we use the resolution of the land/sea mask of the most resolved field, e.g., 0.25°. Errors due to the choice of the land/sea mask have been estimated to be about 5% (Petrov and Boy

2004). Table 1 introduces the spatial and temporal resolutions as well as the coverage of the models we used to compute the motion induced by NTL.

We compute the loading time series for the 585 sites whose observations have passed the quality control (see data section). To compare with daily VLM observed by GPS, we run a daily average on the loading time series when the temporal sampling of the model outputs is less than 24 h. We use the sub-daily motions to estimate the daily variability for the predicted VLM.

Non-tidal atmospheric loading

We compute NTAL effects using surface-pressure fields provided by the latest operational model of the European Centre for Medium-range Weather Forecasts (ECMWF). These surface-pressure fields have a temporal sampling of 3 h. The spatial resolution of the model evolved over time: from about 0.35° (T511 grid) in 2000 to about 0.25° (T799 grid) in 2006 and finally about 0.15° (T1279 grid) in 2010. As pointed out by Duan et al. (2012), some spurious jumps (in February 2006 and January 2011) appear when the spatial resolution of the ECMWF operational model was upgraded. In most cases, when a significant change is introduced in the model, the old and the new versions of the model are run simultaneously for a few months allowing us to adjust for any bias that may appear.

Computation of NTAL also requires a model describing the ocean response to pressure forces. Generally, the ocean is assumed to follow the inverted barometer (IB) hypothesis, which means that atmospheric pressure variations are fully compensated by static sea height variations (Wunsch and Stammer 1997). A slight improvement has been introduced to ensure the conservation of the total ocean mass, see van Dam and Wahr (1987) and Petrov and Boy (2004). This simple model is typically verified at periods exceeding a few weeks. At higher frequencies, the dynamic ocean response cannot be neglected. To account for the dynamic changes of sea-surface heights, we use the Toulouse Unstructured Grid Ocean model (TUGO-m) (updates of Carrere and Lyard 2003). TUGO-m is a barotropic ocean model which means that constant-pressure (isobaric) surfaces in the ocean are also constant-density (isopycnic) surfaces so that the pressure gradient does not change with depth but only depends

Table 1 List of models used to compute the position changes at GPS sites due to loading and their spatial and temporal resolution

Resolution	ECMWF	TUGO-m	ECCO	GLORYS	GLDAS	MERRA
Space	0.15° to 0.35°	0.25°	0.3° to 1°	0.25°	0.25°	0.5° × 0.67°
Time	3 h	3 h	12 h	24 h	3 h	1 h
Coverage	Global	Global	73° S to 73° N	Global	Global but without permanently snow- and ice-covered regions	

on the sea-surface slope. TUGO-m is forced by the same ECMWF operational surface air pressure and wind fields. This model is run on a finite-element grid and extrapolated to a regular 0.25° grid; the temporal resolution is also 3 h, i.e., equal to the forcing fields.

To summarize, using the static (IB) and the dynamic (D) ocean responses to pressure forcing, we obtain two estimates for the VLM induced by NTAL (see also Mémin et al. 2014b):

- IB-NTAL: ECMWF operational/IB,
- D-NTAOL: ECMWF operational+TUGO-m,

where NTAOL means non-tidal atmospheric and oceanic loading because TUGO-m partly includes NTOL. However, TUGO-m does not model the full oceanic circulation because it is not forced by heat and freshwater fluxes.

Non-tidal oceanic loading

The global oceanic circulation induces global earth deformation (van Dam et al. 2012). To compute the VLM due to NTOL induced by the redistribution of mass within the ocean we use two completely independent GCMs: the Estimating the Circulation and Climate of the Ocean (ECCO run kf080h) project (Wunsch et al. 2009), and the Global Ocean ReanalYsis and Simulation (GLORYS2v3) model (Ferry et al. 2012).

ECCO and GLORYS are both baroclinic models, i.e., the density of ocean layers depends on pressure and temperature leading to a pressure gradient changing with depth. They are forced by winds, heat and freshwater fluxes. There are several differences between these models, but the most important is their spatial sampling: GLORYS is an eddy-permitting model, with a global coverage and a resolution of 0.25°; ECCO has a much coarser resolution from 0.3° to 1° and only cover oceans between 73° S and 73° N, i.e., it does not include the Arctic Ocean. The temporal sampling is 12 and 24 h for ECCO and GLORYS, respectively, and the two models differ by their forcing dataset: GLORYS is forced by ECMWF fields, whereas ECCO is forced by National Centers for Environmental Prediction (NCEP) fields.

Because these ocean GCMs are forced by surface winds, they cannot be combined with TUGO-m. However, ECCO and GLORYS are not forced by surface air pressure and we must add the IB-NTAL explained in the previous section to form the IB-NTAOL. We can, therefore, compare IB-NTAOL using either ECCO or GLORYS with D-NTAOL that employs TUGO-m.

TUGO-m was specifically designed to accurately model high-frequency oceanic variability (periods less than a month), in particular, to correct altimetry records (Carrère and Lyard 2003). OGCMs like ECCO and GLORYS are better designed for modeling longer timescales oceanic variability. The first assumption regarding an optimized atmospheric and non-tidal oceanic loading time series would be to use TUGO-m for a short period and barotropic models for periods larger than a month. Another goal of this research is to show that the combination ECMWF + TUGO-m is sufficient to model loading effects over the entire frequency spectrum, including the seasonal timescales.

Continental hydrology loading

Finally, the loading due to continental hydrology also contributes to surface displacements (van Dam et al. 2001). To have the most complete representation of surface-mass changes, we add to our NTAL and NTOL computations the contribution of the continental water storage using two hydrological models, namely the Global Land Data Assimilation System (GLDAS)/Noah (Rodell et al. 2004) and the Modern Era Retrospective-Analysis (MERRA)-land (Reichle et al. 2011).

Continental water storage variations occur mostly at seasonal timescales; however, since rapid events can occur, we choose to use global hydrology models at their finest spatial and temporal resolutions: 3 h and 0.25° for GLDAS/Noah and 1 h and 0.5°×0.67° for MERRA-land. Since these models are inaccurate for regions permanently covered with ice and snow, we choose to mask these regions out. We also enforced the total water mass conservations, by compensating any loss/gain of water over land by an increase/decrease in sea level in the oceans using a uniform layer of water. We use the full water content, i.e., soil-moisture, snow and also canopy water for GLDAS/Noah. For clarity, we omit to mention "/Noah" and "-land" in the next sections.

Analysis of the loading contributions to the vertical land motion

To investigate the magnitude of loading effects, we assume that NTL deformation is not temporally correlated, and we compute for each site the Weighted root mean square (WRMS) of the daily VLM induced by NTL between 01/2002 and 11/2013, with the daily variability as weights. We map the WRMS in Fig. 1 for a set of 6 model combinations (Table 2). In the next section, the NTAOL models are also combined with hydrological models to perform the analysis of geodetic time series. Also, to better describe the differences between using the different models and because of the atmospheric pressure field distribution, we show in Fig. 2 (top left) the 10° latitude-band averages of the WRMS.

The largest WRMS of the VLM induced by the IB-NTAL are obtained in continental Eurasia where they reach more than 4 mm (Fig. 1, top left). On average, WRMS are larger

Fig. 1 WRMS of the predicted VLM induced by loading effects for IB-NTAL using ECMWF pressure fields (top left), D-NTAOL using TUGO-m (top right), IB-NTAOL using ECCO (middle left), IB-NTAOL using GLORYS2v3 (middle right), IB-NTAL + GLDAS/Noah (bottom left), IB-NTAL + MERRA-land (bottom right)
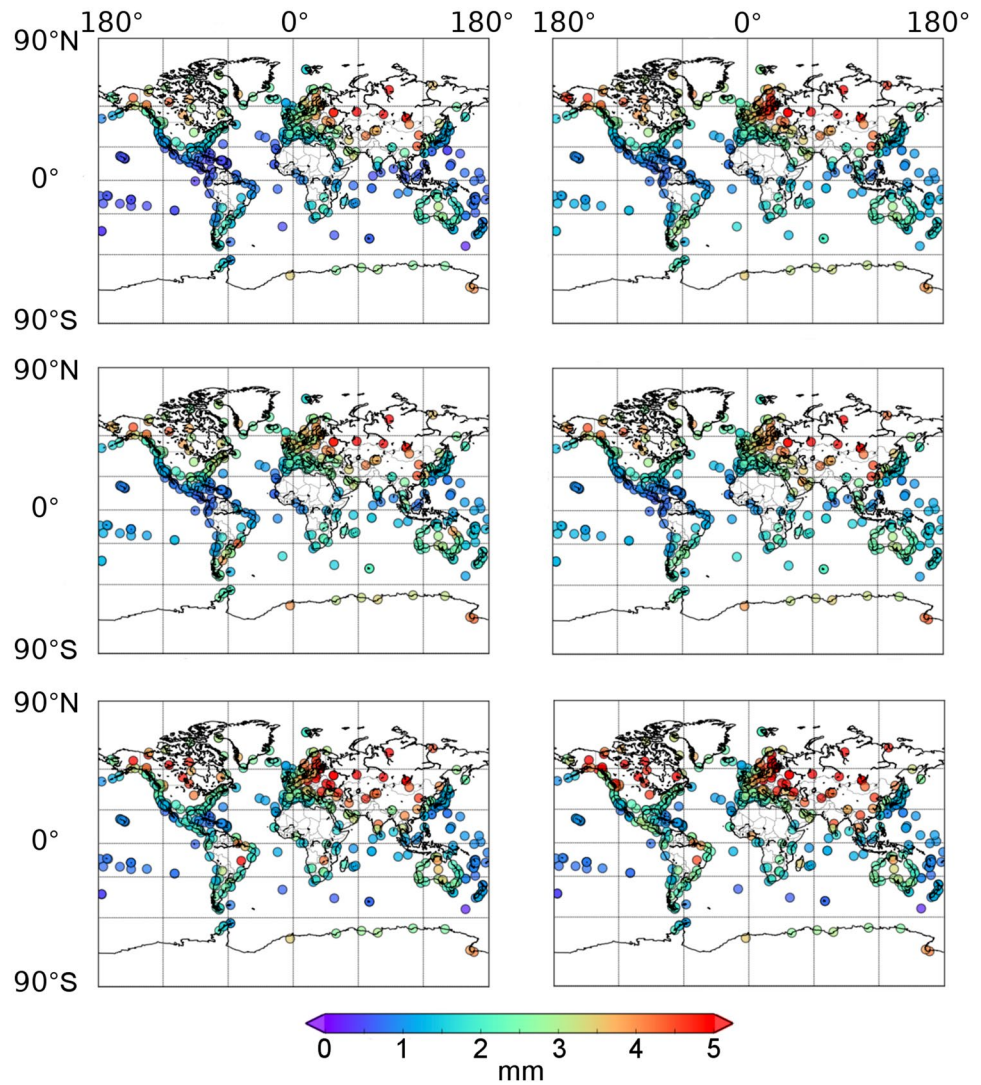

Table 2 List of model combinations used to compute the WRMS of the daily VLM induced by NTL presented in Fig. 1

	ECMWF	IB	TUGO-m	ECCO	GLORYS	GLDAS	MERRA
IB-NTAL	X	X					
D-NTAOL	X		X				
IB-NTAOL/ECCO	X	X		X			
IB-NTAOL/GLORYS	X	X			X		
IB-NTAL/GLDAS	X	X				X	
IB-NTAL/MERRA	X	X					X

than 3 mm for sites within 50 and 70° N and between 70 and 80° S like along the Antarctic coastline, and close to or lower than 1 mm between 20° S and 20° N. There is a clear latitude dependency in WRMS induced by IB-NTAL with a symmetry that is directly connected to the low (high) atmospheric variability at low (high) latitudes. Between 40 and 70° S, the low WRMS (about 1–1.5 mm), compared to that in the Northern hemisphere (≥ 2 mm), predicted at island or coastal sites is the consequence of the IB assumption and

the presence of large open oceans. Indeed, considering the dynamic changes of the ocean topography (D-NTAOL), the WRMS averages are larger, up to about 1.75–2 mm, within the same range of latitudes. It results from the presence of the Antarctic Circumpolar Current (ACC) that is strongly driven by westerly winds. This difference of the VLM induced by IB-NTAL and D-NTAOL (up to about 1 mm) observed between 40 and 70° S is similar to that observed between 50 and 80° N, which corresponds to sites

Fig. 2 WRMS of the predicted VLM induced by loading effects averaged per 10° latitude bands for IB-NTAL using ECMWF pressure fields (black squares), D-NTAOL using TUGO-m (red circles), IB-NTAOL using ECCO (green crosses), IB-NTAOL using GLORYS2v3 (blue crosses), IB-NTAL+GLDAS/Noah (magenta up-pointing triangles) and IB-NTAL+MERRA-land (gray down-pointing triangles). WRMS averages are computed for loading time series with a signal with periods within the entire frequency range (top left), signal with periods longer than 2 months including (middle left) or removing (middle right) the seasonal changes, periods between 1 week and 2 months (bottom left) and periods shorter than 1 week (bottom right)
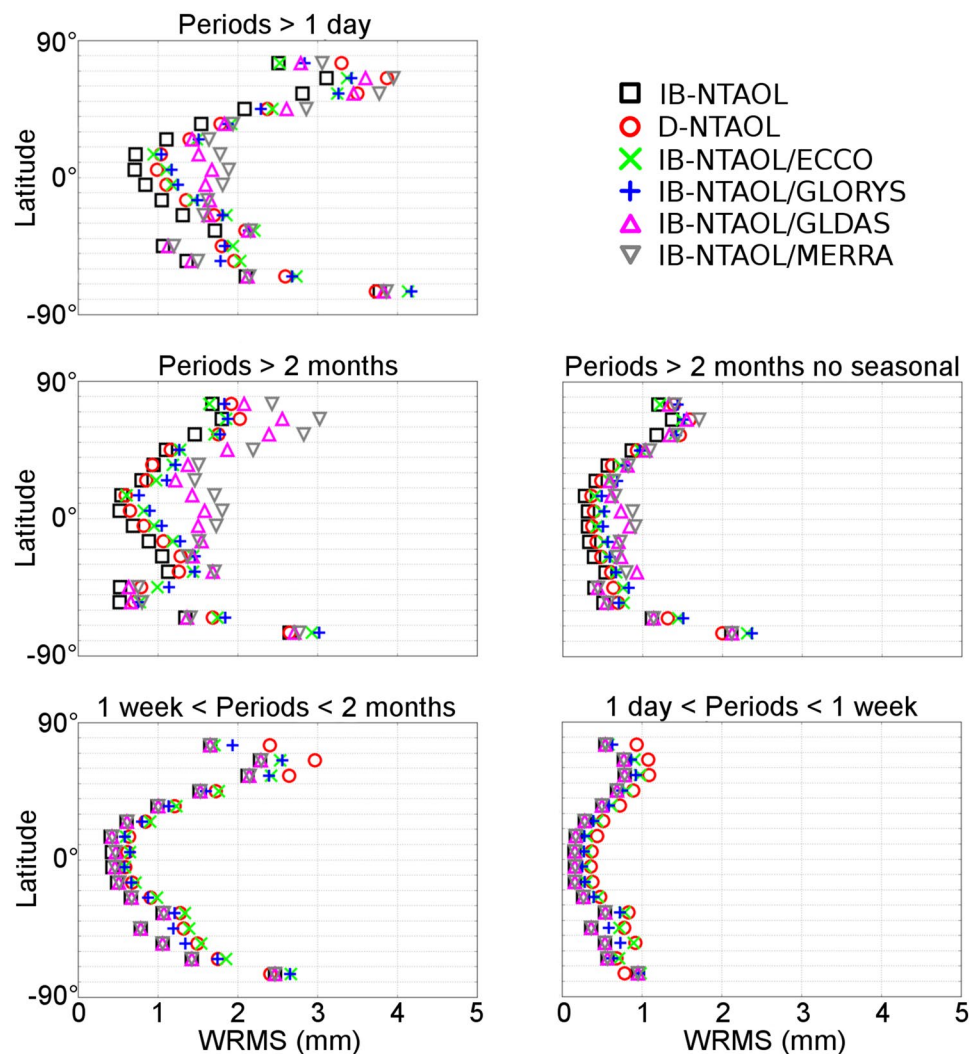
mostly in Scandinavia. This difference is due to high frequencies (periods shorter than 2 months) of ocean variability as represented in TUGO-m that can lead to VLM with WRMS differences reaching up to 1 mm compared to IB-NTAL (Fig. 2-bottom). At other latitudes, using D-NTAOL increases the WRMS averages by less than 0.4 mm. Adding the NTOL contribution to IB-NTAL using either ECCO or GLORYS leads to very similar results (Fig. 2), namely an increase in the WRMS averages at all latitudes by up to 0.7 mm between 40 and 70° S. The only notable difference between using ECCO or GLORYS, on the order of 0.2–0.3 mm, is obtained for sites located north of 70° N. This difference is due to the absence of the Arctic Ocean in ECCO. D-NTAOL leads to the largest WRMS between 50 and 80° N (Fig. 1-top right and middle, Fig. 2-top left)

Adding the hydrological contribution to IB-NTAL also increases, up to 1 mm, the WRMS averages at latitudes North of 40° S. The loading due to hydrology is larger than or equal to NTOL north of 20° S which reflects the influence of the tropical climate within the equatorial band but also the geometrical distribution of the sites given that inland sites are the most affected by hydrology, compare for example Figs. 1 (bottom) with Fig. 1 (top left). Sites located south of 40° S, mostly in South America, New Zealand, and Antarctica, are not significantly affected by the effect of hydrology as represented in the models we used.

To characterize the amplitude of the temporal variability of the NTL, we filter the estimated loading time series and repeat the computation of the WRMS considering several frequency bands: the long-period band above 2 months with and without the annual and semi-annual components, the intermediate-period band with periods between 1 week and 2 months, and the short-period band with periods less than a week. The results are shown in Fig. 2. As expected, we find that IB-NTAL leads to the lowest WRMS averages at all latitudes and for all frequency bands. The largest WRMS averages, reaching up to 2–3 mm, are in the intermediate-period band for NTOL and in the long-period band that includes the

seasonal signal for the loading due to hydrology, MERRA is leading to larger WRMS averages than GLDAS in the northern hemisphere, up to 0.4 mm between 50° N and 70° N. In the short- and intermediate-period bands, D-NTAOL leads to larger WRMS averages than IB-NTAOL and the hydrological loading shows no impact at all. No significant difference is obtained between D-NTAOL and IB-NTAOL in the long-period band in which both show WRMS averages smaller than those induced by hydrological loading but larger on average than 1 mm. Finally, WRMS averages for inter-annual signals, typically the long-period band that does not include the seasonal signal, are larger than 1 mm for sites located north of 40° N and south of 60° S. The motion of stations toward east and north directions (not shown) is much lower than vertical ones, less than 0.6 mm, at all frequencies leading to a maximum displacement, located along the coast of Antarctica, of lower than 0.8 mm. The small differences between D-NTAOL and IB-NTAOL at long periods mean that loading computation using ECMWF + TUGO-m is able to correctly represent seasonal displacements, although TUGO-m was specifically designed to model short-period oceanic circulation.

Loading effects in observed vertical displacements at GPS sites

In this section, we assess if and investigate how the WRMS of the vertical positioning time series determined by GPS can be reduced by applying a posteriori the predicted vertical displacements induced by NTL.

GPS data and processing

GPS data processing was carried out using double-differenced ionospheric-free GPS phase observations with the GAMIT software version 10.5 (Herring et al. 2010). The standard IERS/IGS (repro2 campaign) models and corrections were applied. A priori hydrostatic zenith tropospheric delay values were extracted from the VMF1 grids (Boehm et al. 2006). Residual wet zenith tropospheric delays were adjusted at 1 h intervals for every station using a piecewise linear model. Both the hydrostatic and wet VMF1 mapping functions were used. The azimuthal asymmetry in the tropospheric delay was accounted for by estimating two atmospheric gradients for each day and station using the mapping function developed by Chen and Herring (1997). The corresponding motions of the crust due to solid earth and pole tides (solid earth and ocean) were corrected following the International Earth Rotation and Reference Systems Service (IERS) Conventions (Petit and Luzum, 2010). Crustal motion due to the ocean tide loading was corrected by interpolating the tidal constituents at each station from

the FES2004 model (Lyard et al. 2006). Loading due to atmospheric tides was not corrected. No non-tidal loading corrections (atmospheric, oceanic, hydrology) were applied.

From the 757 stations of the ULR6 solution (Santamaría-Gómez et al. 2017), we select time series of daily station positions derived from GPS data, which are longer than 1 year with at least 100 samples. This results in 585 time series. We analyze the time series using a two-stage process to mitigate the influence of outliers. We first pre-process the time series to remove all data with formal errors exceeding a threshold of 15 mm. Second, we fit each time series to a model that includes mean offset, trend, periodic components, including solar annual and semi-annual periods and the GPS draconitic year (351.4 days), and position offsets using weighted least squares. We correct the time series for the adjusted model and discard from the time series samples greater than 3 times the standard deviation of the residuals. Our processing leads to a sample rejection of ≤ 10% of the initial data for 90% of the 585 selected time series. The periodic variations of the model are then restored to the time series.

Figures 3 and 4 depict some statistics about the selected VLM time series. An apparent asymmetry exists between the two hemispheres (Fig. 3) where 73% of our selected time series are for sites located in the northern hemisphere. For instance, about 29% of the sites are between 40° N and 60° N, 19% are between −20° N and 20° N, and ≤ 1.7% are north 70° N or south 70° S. Despite this asymmetry in the meridional distribution of sites, a strong dependency on latitudes exists in the WRMS of the VLM time series. Indeed, the averaged WRMS is about 7 mm at high latitudes, decreasing down to about 5–6 mm at mid-latitudes and increasing within the tropical band [−20° N–20° N] to reach the largest WRMS about the equator ≥ 8 mm (Fig. 4). Similar behavior is observed for the root mean square (RMS) of the VLM
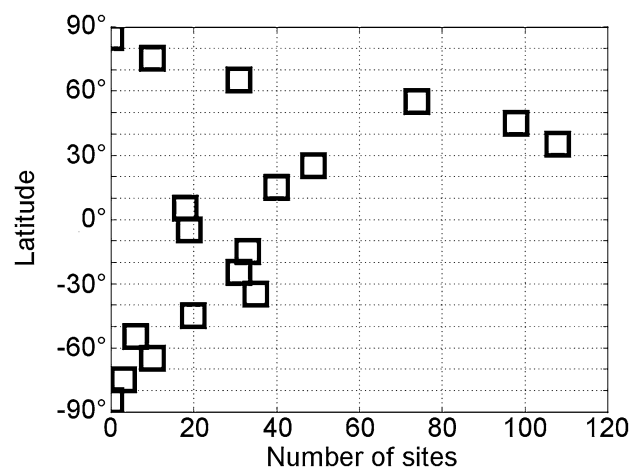
Fig. 3 Meridional average (10°) of the distribution of GPS sites
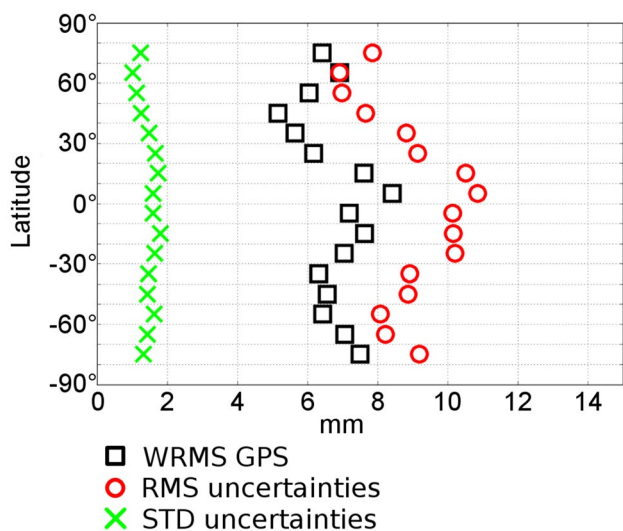
Fig. 4 Meridional average (10°) of statistics of the 585 VLM time series obtained from ULR solutions: WRMS of VLM time series (black squares), RMS of VLM uncertainties (red circles) and standard deviation (STD) of VLM uncertainties (green crosses)

uncertainties. However, the magnitude is about 2 mm larger at all latitudes but latitudes north and south of 50° N and 50° S, respectively. Between 60° N and 70° N, the RMS of VLM uncertainties are almost identical to WRMS of the VLM time series. The VLM uncertainties are also subject to time variability given that their standard deviation (STD), which also depends on latitudes, is in the range of 1 and 2 mm. Repeating the analysis (not shown) for the east and north land motion (E-NLM) reveals that the WRMS of time series range between 2 and 3 mm, RMS and STD of E-NLM uncertainties are about 3–4 mm and ≤ 1 mm, respectively. The clear latitude dependency observed in VLM is much less pronounced, ≤ 1 mm in ELM, or absent in NLM.

Figure 5 shows the site distribution for the length of the VLM time series obtained from ULR solutions and for the number of time samples (very similar plots, not shown, are obtained for ELM and NLM). The figure shows that the length of the time series is longer than 10 years for about half of the sites and that at most sites (≥ 90%), and the length is longer than 4 years with more than 1000 time samples.

Observed and predicted vertical land motion

To assess the effect of NTL and its frequency content on observed VLM time series, we quantify the WRMS reduction of the observed VLM series from the ULR 6 solution when we apply NTL corrections. We first start correcting the observed VLM series for predicted VLM derived from long-period (≥ 2 months) NTL corrections, excluding seasonal changes. We model, using a least-square fit, the seasonal signal and remove it from predicted VLM. For IB-NTAL/
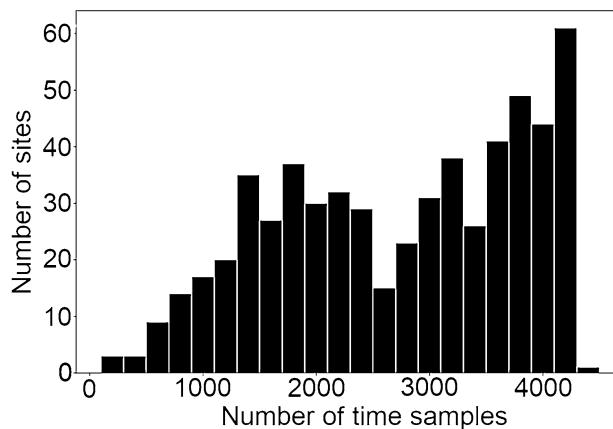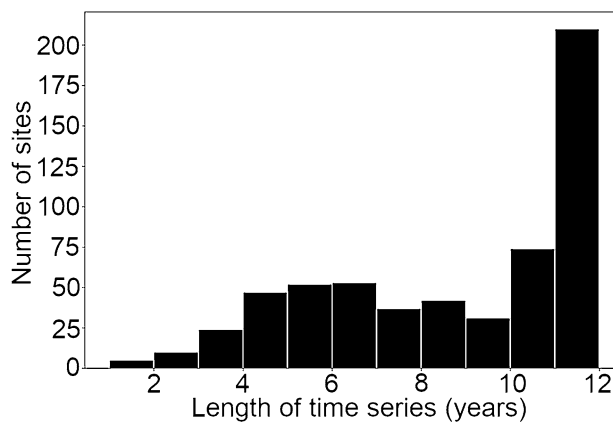

Fig. 5 Site distribution of the length of the VLM time series obtained from ULR solutions (top) and of the number of time samples (bottom)

NTAOL and D-NTAOL, the largest mean WRMS reduction of about 5% is obtained for sites located along the coast of Antarctica while it is half of that for sites north of 50° N (Fig. 6-top left), and there is no reduction between − 60° N and 50° N. There is no further significant reduction by adding hydrology loading correction using either MERRA or GLDAS (Fig. 6- middle and bottom left). Then, we progressively increase the frequency content of the predicted VLM. No filter has been applied to the observed VLM for this study.

Second, we further remove the modeled seasonal loading signal from the observed VLM time series (Fig. 6-right). The WRMS reduction increases by 1 to 5–6%, reaching 10% in Antarctica (Fig. 6-top right). There are slightly larger reductions correcting for D-NTAOL and IB-NTAOL than for IB-NTAL. Correcting for hydrology loading further reduces the mean WRMS by up to 5% at sites located north of 40°. However, there is no significant difference between using either MERRA or GLDAS (Fig. 6-middle and bottom right).

Third, we correct for loading signals with periods longer than 7 days (Fig. 7-left). The averaged WRMS of VLM time

Fig. 6 Averaged WRMS reduction per 10° latitude bands of VLM observed by GPS when corrected for predicted loading effects for IB-NTAL using ECMWF pressure fields (black squares), D-NTAOL using TUGO-m (red circles), IB-NTAOL using ECCO (green crosses), IB-NTAOL using GLORYS2v3 (blue crosses). Hydrology loading is neglected (top), modeled using GLDAS/Noah (middle), and MERRA-land (bottom). The WRMS reductions are computed for loading time series containing long-period signal only and removing (left) or considering (right) the seasonal variations
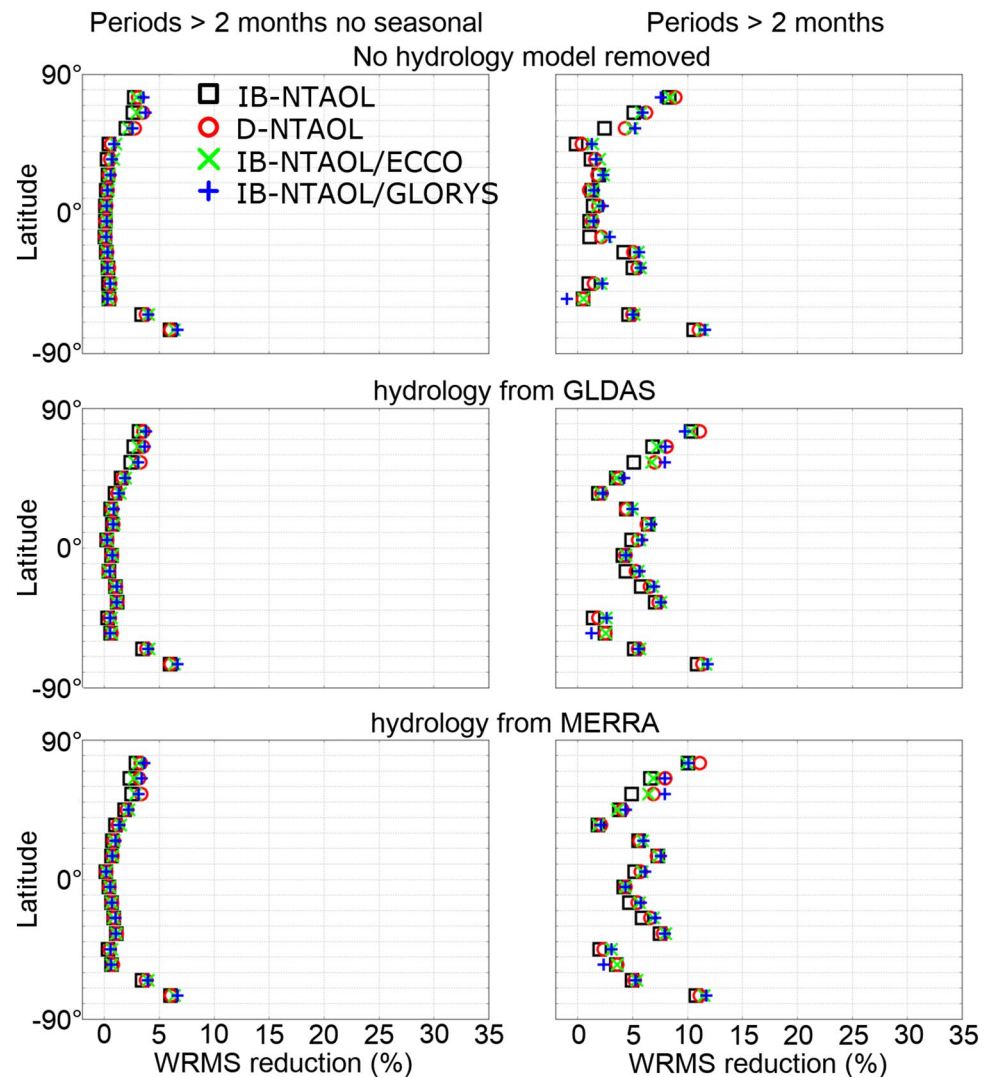
series further reduces by up to 12%. Sites located north of 50° N obtained the largest reduction, up to 20%. On average, IB-NTAL leads to the lowest reductions with differences of a few percent for sites north of 50° N. Finally, correcting for loading signal including short periods (≥ 1 day), so that the whole spectrum is considered (Fig. 7-right), further reduces by up to 2% the averaged WRMS, mostly in the northern hemisphere (north of 30° N). Figure 8 shows the WRMS reduction of observed VLM at all sites corrected for IB-NTAOL using GLORYS and hydrology loading modeled using MERRA-land. The largest reduction is obtained for European and North American sites while small-island sites located south of 60° N systematically have a reduction ≤ 8–10%.

A similar analysis for ELM and NLM shows that the averaged WRMS reduction per 10° latitude bands is $\leq 5\%$. The largest reduction is obtained between 50° N and 80° N when including periods ≤ 2 months for ELM, and between 20° N and 30° N for NLM when considering a seasonal signal.

Contrary to VLM, there are no significant changes ($\leq 1\%$) in the WRMS reduction using the different loading models. The largest reductions (≥ 5–6%) for ELM and NLM are obtained for sites along the coast of North America, while small-island sites systematically have a reduction ≤ 1–2%.

Concluding remarks

We compared a set of 585 GPS position time series, globally distributed, with several atmospheric, non-tidal oceanic and hydrological loading models. In particular, we investigate two different models of oceanic response to atmospheric pressure variations: the classical inverted barometer (IB) approximation and the barotropic TUGO-m model. We find that the D-NTAOL (ECMWF + TUGO-m) better agrees with observed vertical surface motion than the more classical IB-NTAL (ECMWF/IB) model. The variance of observed VLM using the D-NTAOL model compared to

Fig. 7 Averaged WRMS reduction per 10° latitude bands of VLM observed by GPS when corrected for predicted loading effects for IB-NTAL using ECMWF pressure fields (black squares), D-NTAOL using TUGO-m (red circles), IB-NTAOL using ECCO (green crosses), IB-NTAOL using GLORYS2v3 (blue crosses). Hydrology loading is neglected (top), modeled using GLDAS/Noah (middle) and MERRA-land (bottom). WRMS reductions are computed for loading time series containing periods ≥ 2 months (left) and ≥ 1 day (right)
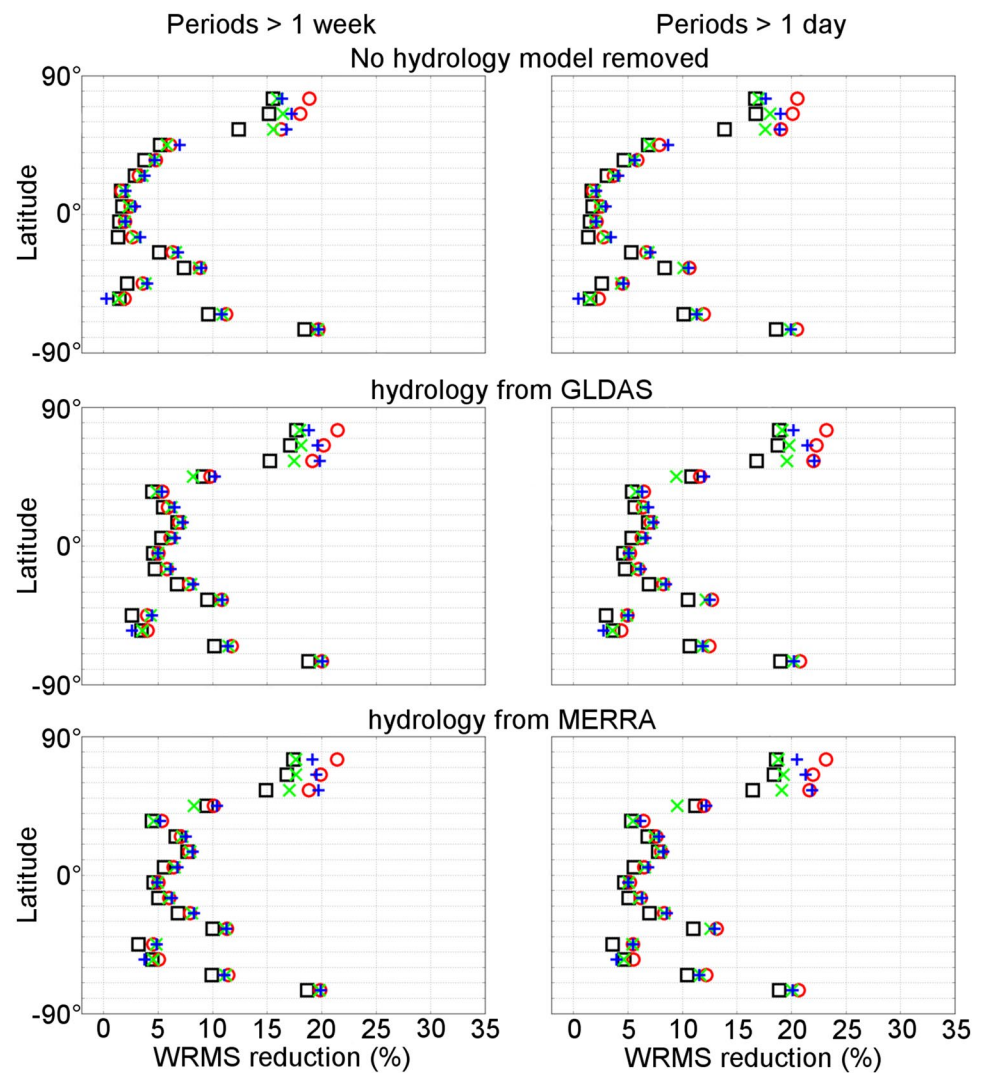
the classical IB-NTAL is reduced in all frequency bands, i.e., for periods from 1-day to several years. This proves that the TUGO-m model is more appropriate for modeling atmospheric and induced oceanic (response to air-pressure) loading effects than the classical IB assumption.

In addition, there is no clear improvement using a baroclinic ocean general circulation model (GLORYS or ECCO here) compared to the barotropic TUGO-m model, even at seasonal timescales. This means that our D-NTAOL (ECMWF/TUGO-m) loading model is also appropriate for modeling loading effects due to changes in the atmosphere and the ocean (response to air pressure and classical oceanic circulation) at all periods.

The comparison of atmospheric and oceanic loading models with observed GPS vertical displacements showed that the TUGO-m model is more appropriate than the classical IB assumption at short period. We also showed that there are no clear differences between TUGO-m and baroclinic ocean models (GLORYS and ECCO) at longer timescales

(monthly to seasonal). Therefore, we recommend the use of TUGO-m in addition to ECMWF surface pressure to model the atmospheric and oceanic loading effects over the entire spectrum.

Adding continental hydrology loading models, using either MERRA-land or GLDAS/Noah, helps improve the agreement between VLM observations and loading estimates at seasonal timescales only. We cannot distinguish the differences between these models using GPS observations. The sum of atmospheric, oceanic and hydrological (D-NTAOL + GLDAS/Noah or MERRA-land) loading models cannot explain the large variability of GPS observations, even at annual timescales. For the seasonal frequencies, this can be due to some components of the hydrological cycle that are not represented in most global hydrological models, e.g., surface waters (lakes, reservoirs, and rivers) and groundwater. Despite its coarser temporal resolution (1 month compared to 3 h), continental water storage derived from the gravity mission GRACE (Gravity Recovery And Climate
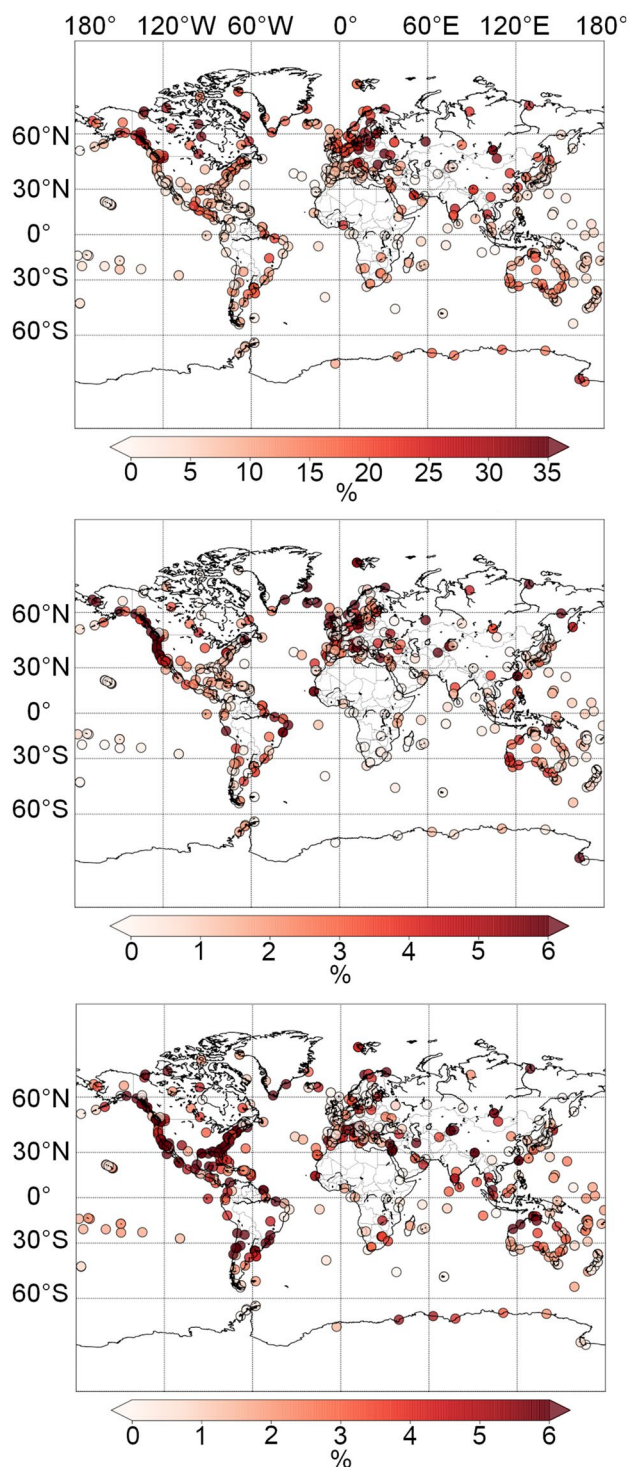
Fig. 8 WRMS reduction of VLM (top), ELM (middle) and NLM (bottom) observed by GPS when corrected for IB-NTAOL using GLORYS2v3 and hydrology loading modeled using MERRA-land

Experiment - Tapley et al. 2004; Davis et al. 2004) might improve the agreement between modeled and observed VLM.

The large part of the GPS variability, especially at low latitudes, cannot be explained by loading effects. One reasonable cause of this might be the mismodeled tropospheric delay. In particular, the atmospheric circulation in the equatorial band is characterized by rapid dynamic phenomena that cannot be captured by global models with a horizontal resolution of a few tens of kilometers and temporal resolutions of 3 to 6 h. Also, considering the atmosphere as a non-isotropic medium instead of an isotropic one as it is done in classical mapping functions (Desjardins et al. 2016), should lead to a reduced VLM variability and an improved agreement between observations and loading models.

References

Blewitt G (2003) Self-consistency in reference frames, geocenter definition, and surface loading of the solid Earth. J Geophys Res 108(B2):2103. https://doi.org/10.1029/2002JB002082

Boehm J, Werl B, Schuh H (2006) Troposphere mapping functions for GPS and very long baseline interferometry from European Centre for Medium-Range Weather Forecasts operational analysis data. J Geophys Res 111:B02406

Boehm J, Heinkelmann R, Mendes Cerveira PJ, Pany A, Schuh H (2009) Atmospheric loading corrections at the observation level in VLBI analysis. J Geod 83:1107–1113. https://doi.org/10.1007/s00190-009-0329-y

Carrère C, Lyard F (2003) Modelling the barotropic response of the global ocean to atmospheric wind and pressure forcing—comparisons with observations. Geophys Res Lett 30(6):1275. https://doi.org/10.1029/2002GL016473

Chen G, Herring TA (1997) Effects of atmospheric azimuthal asymmetry on the analysis of space geodetic data. J Geophys Res 102:20489–20502

Collilieux X, Altamimi Z, Coulot D, van Dam T, Ray J (2010) Impact of loading effects on determination of the international terrestrial reference frame. Adv Space Res 45(4):144–154. https://doi.org/10.1016/j.asr.2009.08.024

Davis JL, Elósegui P, Mitrovica JX, Tamisiea ME (2004) Climate-driven deformation of the solid Earth from GRACE and GPS. Geophys Res Lett. https://doi.org/10.1029/2004gl021435

Desjardins C, Gegout P, Soudarin L, Biancale R (2016) Rigorous interpolation of atmospheric state parameter for ray-traced tropospheric delays. In: Sneeuw N, Novák P, Crespi M, Sansò F (eds) VIII Hotine-marussi symposium on mathematical geodesy, vol International Association of Geodesy Symposia, 142nd edn. Springer, Cham, pp 139–146. https://doi.org/10.1007/1345.2015.10

Duan J, Shum CK, Guo J, Huang Z (2012) Uncovered spurious jumps in the GRACE atmospheric de-aliasing data: potential contamination of GRACE observed mass change. Geophys J Int 191(1):83–87. https://doi.org/10.1007/s00190-009-0327-0

Eriksson D, MacMillan DS (2014) Continental hydrology loading observed by VLBI measurements. J Geod 88(7):675–690. https://doi.org/10.1007/s00190-014-0713-0

Farrell WE (1972) Deformation of the Earth by surface loads. Rev Geophys Space Phys 10:761–797

Ferry N et al (2012) GLORYS2V1 global ocean reanalysis of the altimetric era (1993–2009) at mesoscale. Merc Ocean-Q Newsl 44:10

Fratepietro F, Baker TF, Williams SDP, Van Camp M (2006) Ocean loading deformations caused by storm surges on the northwest European shelf. Geophys Res Lett. https://doi.org/10.1029/2005gl025475

Gégout P, Boy JP, Hinderer J, Ferhat G (2010) Modeling and observation of loading contribution to time-variable GPS sites positions. Int Assoc Geod Symp 135(8):651–959. https://doi.org/10.1007/978-3-642-10634-786

Geng J, Williams SDP, Teferle FN, Dodson AH (2012) Detecting storm surge loading deformations around the southern North Sea using subdaily GPS. Geophys J Int 191(2):569–578. https://doi.org/10.1111/j.1365-246X.2012.05656.x

Herring TA, King RW, McClusky SC (2010) Introduction to GAMIT-GLOBK. Massachusetts Institute of Technology, Cambridge, p 48

Jiang W, Li Z, van Dam T, Ding W (2013) Comparative analysis of different environmental loading methods and their impacts on the GPS height time series. J Geod 87(7):687–703. https://doi.org/10.1007/s00190-013-0642-3

Krásná H, Malkin Z, Böhm J (2015) Non-linear VLBI station motions and their impact on the celestial reference frame and Earth orientation parameters. J Geod 89(10):1019–1033. https://doi.org/10.1007/s00190-015-0830-4

Lyard F, Lefevre F, Letellier T, Francis O (2006) Modelling the global ocean tides: modern insights from FES2004. Ocean Dynam 56:394–415

MacMillan DS, Gipson JM (1994) Atmospheric pressure loading parameters from very long baseline interferometry observations. J Geophys Res 99(B9):18081–18087

Mangiarotti S, Cazenave A, Soudarin L, Crétaux JF (2001) Annual vertical crustal motions predicted from surface mass redistribution and observed by space geodesy. J Geophys Res 106(B3):4277–4291

Mémin A, Rogister Y, Hinderer J, Llubes M, Berthier E, Boy JP (2009) Ground deformation and gravity variations modelled from present-day ice thinning in the vicinity of glaciers. J Geodyn 48(3–5):195–203. https://doi.org/10.1016/j.jog.2009.09.006

Mémin A, Spada G, Boy JP, Rogister Y, Hinderer J (2014a) Decadal geodetic variations in Ny-Ålesund (Svalbard): role of past and present ice-mass changes. Geophys J Int 198(1):285–297. https://doi.org/10.1093/gji/ggu134

Mémin A, Watson C, Haigh I, MacPherson L, Tregoning P (2014b) Non-linear motions at Australian geodetic stations induced by non-tidal ocean loading and the passage of tropical cyclones. J Geod 88(10):927–940. https://doi.org/10.1007/s00190-014-0734-8

Petit G, Luzum B (2010) IERS Conventions (2010) IERS Technical Note No. 36, Verlag des Bundesamtes für Kartographie und Geodäsie Frankfurt am Main, pp 179

Petrov L, Boy J (2004) Study of the atmospheric pressure loading signal in very long baseline interferometry observations. J Geophys Res Solid Earth. https://doi.org/10.1029/2003jb002500

Plag HP et al (2009) The goals, achievements, and tools of modern geodesy. In: Plag HP, Pearlman M (eds) Global geodetic observing system. Springer, Berlin

Reichle RH, Koster RD, De Lannoy GJM, Forman BA, Liu Q, Mahanama SPP, Toure A (2011) Assessment and enhancement of merra land surface hydrology estimates. J Climate 24:6322–6338. https://doi.org/10.1007/s10291-011-0248-2

Rodell M et al (2004) The global land data assimilation system. Bull Am Meteor Soc 85(3):381–394

Santamaría-Gómez A, Mémin A (2015) Geodetic secular velocity errors due to interannual surface loading deformation. Geophys J Int Exp Lett 202(2):763–767. https://doi.org/10.1093/gji/ggv190

Santamaría-Gómez A, Gravelle M, Dangendorf S, Marcos M, Spada G, Wöppelmann G (2017) Uncertainty of the 20th century sea-level rise due to vertical land motion errors. Earth Planet Sci Lett 473:24–32

Schuh H, Estermann G, Crétaux JF, Bergé-Nguyen M, van Dam T (2003) Investigation of hydrological and atmospheric loading by space geodetic techniques. In: C Hwang, CK Shum, JC Li (eds) IAG Proceedings, vol 126, pp 123–132, International Workshop on Satellite Altimetry

Sósnica K, Thaller D, Dach R, Jäggi A, Beutler G (2013) Impact of loading displacements on SLR-derived parameters and on the consistency between GNSS and SLR results. J Geod 87(8):751–769. https://doi.org/10.1007/s00190-013-0644-1

Tapley BD, Bettadpur S, Watkins M, Reigber C (2004) The gravity recovery and climate experiment: mission overview and early results. Geophys Res Lett. https://doi.org/10.1029/2004gl019920

Tesmer V, Steigenberger P, Rothacher M, Boehm J, Meisel B (2009) Annual deformation signals from homogeneously reprocessed VLBI and GPS height time series. J Geod 83(10):973–988. https://doi.org/10.1007/s00190-009-0316-3

Tregoning P, van Dam TM (2005) Atmospheric pressure loading corrections applied to GPS data at the observation level. Geophys Res Lett. https://doi.org/10.1029/2005gl024104

Tregoning P, Watson C (2009) Atmospheric effects and spurious signals in GPS analyses. J Geophys Res. https://doi.org/10.1029/2009jb006344

Tregoning P, Watson C (2011) Correction to "Atmospheric effects and spurious signals in GPS analyses". J Geophys Res. https://doi.org/10.1029/2010jb008157

Tregoning P, Watson C, Ramillien G, McQueen H, Zhang J (2009) Detecting hydrologic deformation using GRACE and GPS. Geophys Res Lett. https://doi.org/10.1029/2009gl038718

van Dam TM, Herring TA (1994) Detection of atmospheric pressure loading using very long baseline interferometry measurements. J Geophys Res 99(B3):4505–4517

van Dam TM, Wahr JM (1987) Displacements of the Earth's surface due to atmospheric loading: effects on gravity and baseline measurements. J Geophys Res 92(B2):1281–1286

van Dam TM, Blewitt G, Heflin MB (1994) Atmospheric pressure loading effects on Global Positioning System coordinate determinations. J Geophys Res 99(B12):23939–23950

van Dam T, Wahr J, Milly PCD, Shmakin AB, Lavallée BD, Larson KM (2001) Crustal displacements due to continental water loading. Geophys Res Lett 28(4):651–654

van Dam TM, Wahr JM, Lavallée D (2007) A comparison of annual vertical crustal displacements from GPS and gravity recovery and climate experiment (GRACE) over Europe. J Geophys Res. https://doi.org/10.1029/2006jb004335

van Dam TM, Collilieux X, Altamimi Z, Ray J (2012) Non-tidal ocean loading: amplitudes and potential effects in GPS height time series. J Geod 86(11):1043–1057. https://doi.org/10.1007/s00190-012-0564-5

Wunsch C, Stammer D (1997) Atmospheric loading and the oceanic "inverted barometer" effect. Rev Geophys 31(1):79–107

Williams SDP, Penna NT (2011) Non-tidal ocean loading effects on geodetic GPS heights. Geophys Res Lett. https://doi.org/10.1029/2011gl046940

Wunsch C, Heimbach P, Ponte R, Fukumori I, the ECCO-GODAE Consortium Members (2009) The global general circulation of the ocean estimated by the ECCO-consortium. Oceanog 22(2):88–103

Anthony Mémin received his PhD in gravimetry and geodesy from Université de Strasbourg, France, in 2011. He is an Associate Professor at Université Côte d'Azur, Nice, France, since 2014. He studies the response of the solid Earth in terms of surface deformation and gravity variations induced by daily to millennia surface-mass redistributions.

Alvaro Santamaría-Gómez received his PhD in geodesy from the Astronomy and Astrophysics Doctoral School of Paris, France, in 2010. He is an Associate Professor at the Paul Sabatier University and the Observatoire Midi-Pyrénées where he oversees the GNSS RENAG network in the Pyrenees. His research focuses on earth surface deformation using GNSS observations.

Jean-Paul Boy is a full professor at EOST/IPGS at the University of Strasbourg. He is currently the director of the Central Bureau of the International Geodynamics and Earth Tide Service (IGETS) and the chair of the Global Geophysical Fluid Center.